Monitoring of Winter Wheat Powdery Mildew Using Satellite Image Time Series

Huiqin Ma [1,2], Wenjiang Huang [2,*], Giovanni Laneve [3], Yue Shi [2,4], Linyi Liu [2,4], Qiong Zheng [2,5]

1. School of Applied Meteorology, Nanjing University of Information Science & Technology, Nanjing 210044, China
2. Key Laboratory of Digital Earth Science, Institute of Remote Sensing and Digital Earth, Chinese Academy of Sciences, Beijing 100094, China
3. Sapienza Università di Roma. Scuola di Ingegneria Aerospaziale
4. University of Chinese Academy of Sciences, Beijing 100049, China
5. College of Geosciences and Surveying Engineering, China University of Mining and Technology, Beijing, 100083, China

Introduction

Powdery mildew (*Blumeria graminis*) is one of the most destructive foliar diseases of winter wheat and its infection results in a reduction of yield and quality. Powdery mildew can infect wheat in the whole growth period. However, the current studies on crop diseases were mostly based on one single growth phase image in late stage of disease development, did not consider the temporal change characteristics of diseased crops.

The objective of this study were to: 1) analyze the relationship between index (NDVI and EVI) time series and winter wheat powdery mildew development, 2) monitor the occurrence severity of disease through NDVI and EVI time series, 3) map the spatial distribution of disease, and 4) assess the performance of the proposed disease monitor model.

Materials and Methods

Study area and disease field survey

The study area is located in western Guanzhong plain in Shaanxi Province, China (**Figure 1**). Located the main high-yield farming area with good hydro-thermal conditions and mild and humid climate conditions. Winter wheat is a major local crop, and the area provides a suitable propagating and developing environment for the powdery mildew pathogen. Two typical disease infected regions (region 1 and region 2) were chosen for disease field observation.

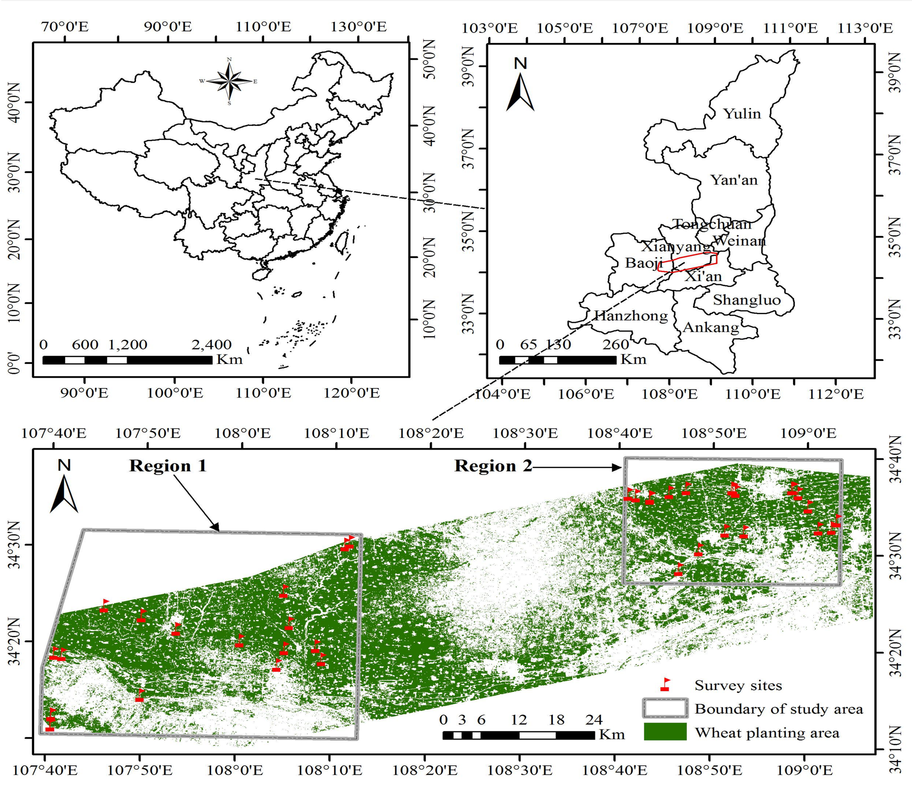

Figure 1. Geographic location and spatial distribution of filed sample points.

Total 42 field survey plots were collected in region 1 and region 2, respectively (**Table1**). the disease occurrence severity was reclassified into three levels (normal, slight, severe) to reduce the difficulty of monitoring.

Table 1. Basic information for disease survey experiment.

Location	Number of field survey samples			
	Normal	Slight	Severe	Sum
Region 1	5	11	5	21
Region 2	17	4	0	21

Remote sensing data acquisition and processing

Total 18 images were acquired, for the period from 16th November 2013 to 9th April 2014. In order to reduce the impact of cloud cover, three sensors' data were chosen to form VIs time series with relatively uniform time intervals (**Table 2**).

Table 2. Information of imagery for disease monitoring.

Platform	Landsat-8	HJ-1A/1B	GF-1
Sensor	LOI	CCD	WFV
Image amount	7	5	6
Spatial resolution	30 m	30 m	16 m
Image swath	180 km	360 km	800 km
Revisit time	16 days	4 days	4 days

Research methods

Many features associated with wheat characteristics and habitat traits based on satellite imagery were rapidly developed and widely used, but almost all these studies focused on the detection and monitoring in the late infection development stage using single-date image. However, time series imagery have been successfully applied to the detection of the tree diseases and pests.

A) Index characteristics

NDVI is sensitive to green vegetation and EVI can reduce the adverse effects of environmental factors.

$$NDVI = \frac{\rho_{nir} - \rho_{red}}{\rho_{nir} + \rho_{red}}$$

$$EVI = G \times \frac{\rho_{nir} - \rho_{red}}{\rho_{nir} + (C_1 \times \rho_{red} - C_2 \times \rho_{blue}) + L}$$

B) Discrete wavelet transform (DWT)

The imagery were influenced by noise such as cloud cover and image acquisition platforms. Hence, DWT was used to denoised to obtain final NDVI and EVI time series features.

C) SVM classifier

SVM largely overcomes the problems of dimensionality disaster and over-study, it has been widely used in recognition and classification, etc.

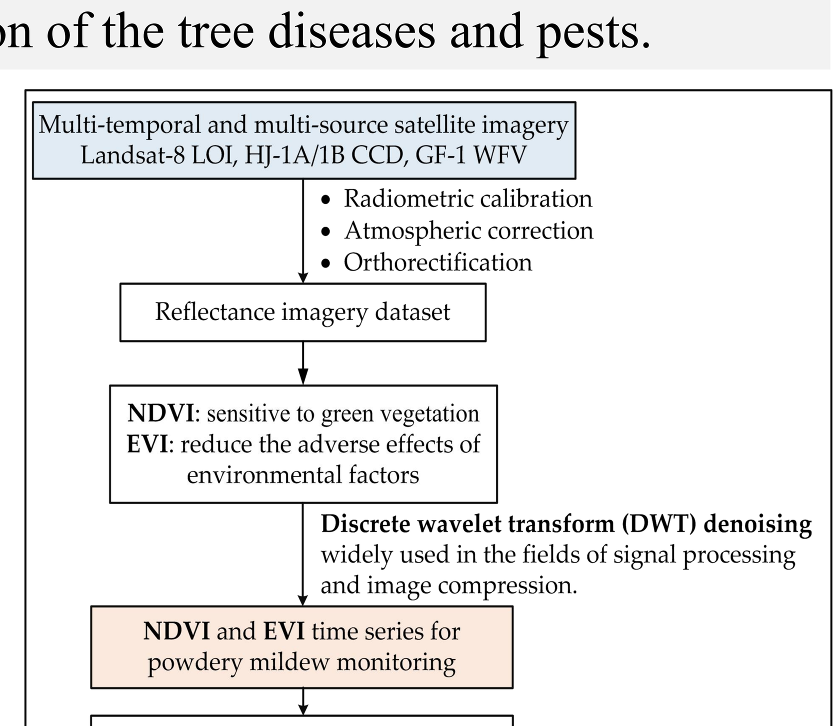

Figure 2. Flowchart of constructing the powdery mildew monitoring models.

Due to the small sample size, **a leave one-out cross validation method** was used to verify the SVM model.

Results and discussion

Powdery mildew runs through the entire wheat growth period from infestation to manifestation. So we assume that the remote sensing images of early critical infection stages of powdery mildew in winter wheat contained some useful information about early disease infection. The original NDVI and EVI time series curves (**Figure 3a, 3c**) are with obvious noise, and the curves of NDVI and EVI time series denoised by DWT (**Figure 3b, 3d**) were significantly smoother than the original VIs time series. The temporal variation of NDVI and EVI indicies of three levels severities powdery mildew infected wheat showed that the overall trend of the three changes were basically the same, but with different details.

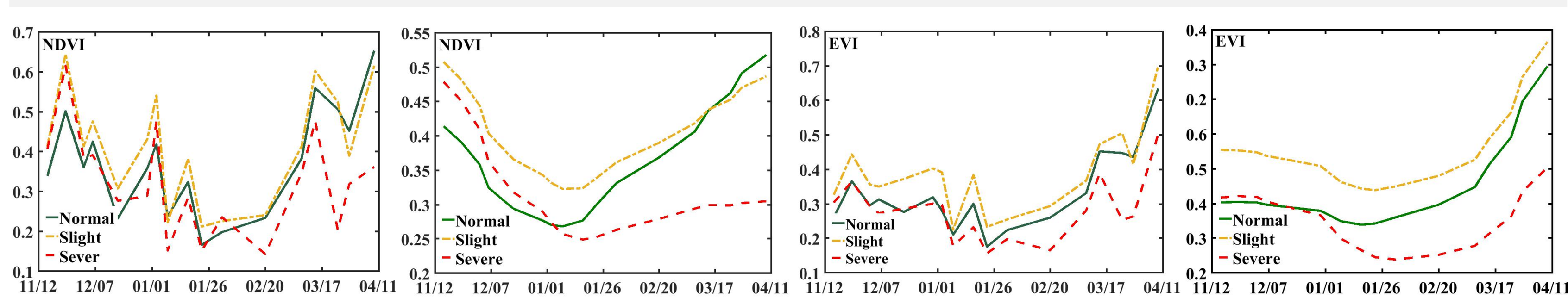

(a) Original NDVI (b) DWT_NDVI (c) Original EVI (D) DWT_EVI

Figure 3. Charictoristics of disease severity infected time series.

NDVI and EVI time series models were applied to the entire study area to monitor the occurrence severity of disease (**Figure 4**). In NDVI time series models, slightly powdery mildew infected wheat basically covered the whole area of region 1. In region 2, winter wheat was almost normal. The powdery mildew infected wheat were distributed largely in both region 1 and 2 in EVI time series model maps.

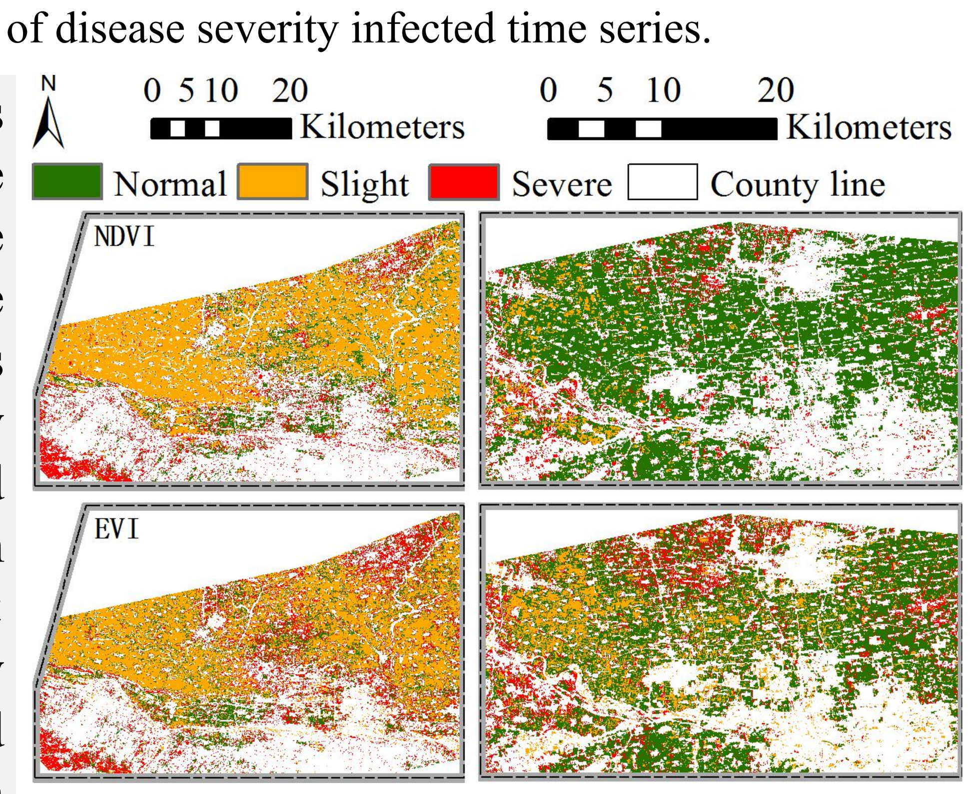

Figure 4. Disease severity spatial distruibution of NDVI and EVI time series DWT-SVM models.

The confusion matrix, users' accuracy (U), producers' accuracy (P), overall accuracy (OA) and Kappa coefficient of the predictive models of severity of wheat powdery mildew associated with VIs time series are listed in **Table 3**. EVI time series model has higher OA of 92.9% and Kappa of 0.88 than NDVI time series model (with OA of 81.0% and Kappa of 0.66).

Compared with disease severity maps (**Figure 4**) and filed survey truth (**Table 1**), the monitoring results were all close to the filed truth in region 1, but the disease area in region 2 may be over evaluated. Furthermore, in order to assess mapping results, the disease severity of time series monitoring maps and the field truth was counted (**Table 4**). Normal and slightly infected wheat were both underestimated, and severely infected wheat was overestimated, but the monitoring reslut of NDVI model was closer the ground truth than EVI model though EVI model had an higher overall accuracy.

Table 3. Confusion matrix and accuracy assessment of the SVM monitoring models with NDVI and EVI time series.

Monitoring		Ground truth			U (%)	OA (%)	Kappa
		Normal	Slight	Severe			
NDVI	Normal	21	1	0	95.5	81.0	0.66
	Slight	5	9	1	60.0		
	Severe	1	0	4	80.0		
	P (%)	77.8	90.0	80.0			
EVI	Normal	21	1	0	95.5	92.9	0.88
	Slight	2	13	0	86.7		
	Severe	0	0	5	100.0		
	P (%)	91.3	92.9	100.0			

Table 4. The disease level ratio of NDVI and EVI time series monitoring maps and the field truth.

Model and field truth	Ratio of disease infection		
	Normal	Slight	Severe
NDVI	48.5%	35.0%	16.5%
EVI	36.2%	33.4%	30.4%
Field truth	52.4%	35.7%	11.9%

Contact: Huiqin Ma
Email: mahq0712@nuist.edu.cn

Conclusion

1. The difference between NDVI and EVI time series curves of wheat infected with different disease severities was obvious.
2. Both the accuracies of the NDVI and EVI time series models suggested that two time series preformed good in quantifying disease severity, but the EVI time series achieved a higher monitor accuracy.
3. The monitoring models with NDVI and EVI time series denoised by DWT outperformed the models with original time series.